Science and Technology Infusion Climate Bulletin
NOAA's National Weather Service
36th NOAA Annual Climate Diagnostics and Prediction Workshop
Fort Worth, TX, 3-6 October 2011

A Metrics for Boreal Summer Monsoon Intraseasonal Oscillation

June-Yi Lee[1] Bin Wang[1] Matthew Wheeler[2], Xiouhua Fu[1] and Duane Waliser[3]

[1]*IPRC and Department of Meteorology, University of Hawaii, USA*

[2]*Centre for Australia Weather and Climate Research, Bureau of Meteorology, Australia*

[3]*Joint Institute for Regional Earth System Science and Engineering, University of California, USA*

1. Introduction

The tropical intraseasonal oscillation (ISO) is one of the most prominent short-term climate variability in the tropics that has a far reaching influence worldwide (Lau and Waliser 2005). In boreal winter, ISO is characterized by the eastward propagating Julian oscillation (MJO) along the equator (Madden and Julian 1972, 1994), which influences a wide range of weather and climate phenomena and may act an important source of predictability at the subseasonal time scale (Lau and Waliser 2005). In boreal summer, northward propagating monsoon ISO (MISO) is prominent at both 10-20 day and 30-60 day periods in the Asian summer monsoon region (Yasunari 1979, 1980; Webster and Hoyos 2004; Kajikawa and Yasunari 2005 and many others). The MISO is more complex in nature than the MJO due to intrinsic monsoon variability as well as the interaction between the basic monsoon circulation and Madden-Julian Oscillation MJO (Webster *et al.* 1998; Lau and Waliser 2005; Wang 2006). The MISO is known to affect summer monsoon onsets, the active/break phases and the seasonal means of summer monsoons. The wet and dry spells of the MISO strongly influence the extreme hydro-meteorological events, which composed of about 80% of natural disaster, thus the socio-economic activities in the World's most populous monsoon region.

The Real-time Multivariate MJO (RMM) index (Wheeler and Hendon 2004) is most widely used the first two leading multi-variate EOF modes of the equatorial mean (between 15ºS and 15ºN) OLR, and zonal winds at 850 and 200 hPa. This index captures equatorial eastward propagating mode, the MJO, very well and has been applied all year around to depict MJO activity. It has been well recognized that the tropical intraseasonal variations exhibits prominent seasonal variation (Madden 1986, Wang and Rui 1990). During boreal summer, the variability centers of OLR are shifted from equatorial zone during boreal winter to off-equatorial monsoon troughs and the

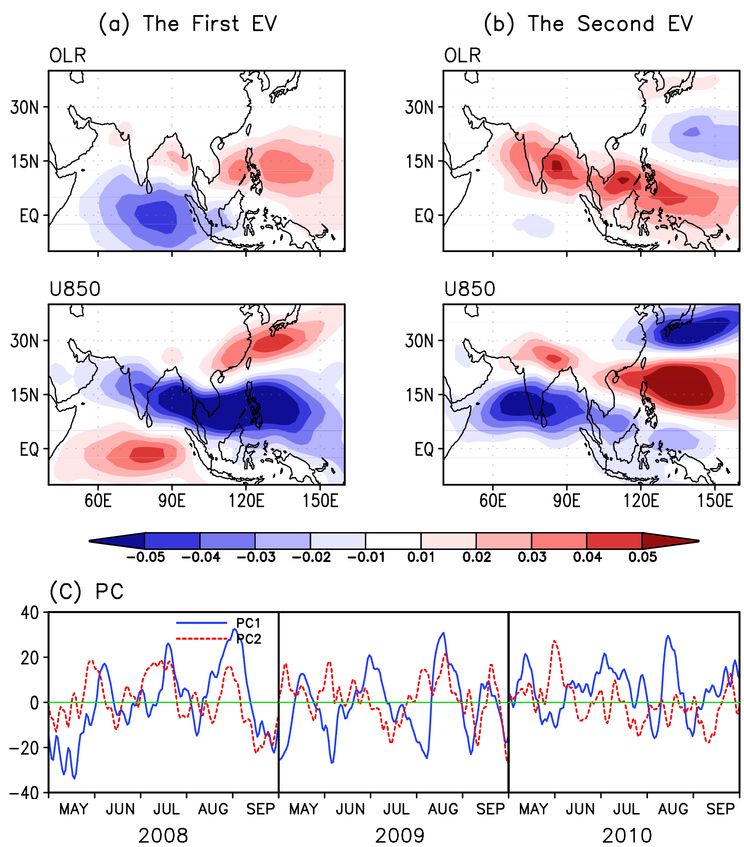

Fig. 1 Spatial pattern (a, b) and PC time series (c) of the first two leading MV-EOF modes of pentad OLR and zonal wind at 850 hPa. In (c), the blue solid line indicates the first and the red dashed line the second principal component (PC). The MV-EOF modes were obtained during MJJAS for the 33 years of 1979-2010.

Correspondence to: June-Yi Lee, Department of Meteorology and International Pacific Research Center, University of Hawaii at Manoa, Honolulu HI 96822; E-mail: juneyi@hawaii.edu.

propagation patterns changed dramatically. It is hence not clear whether RMM remains a best measure of the boreal summer monsoon intraseasonal oscillation (MISO). This study has made an effort on design a better index to describe boreal summer MISO.

2. Definition of MISO index

The data used include interpolated daily outgoing longwave radiation (OLR) with 2.5^{o} horizontal resolution from NOAA (Liebmann and Smith 1996) and daily horizontal wind at 850 and 200 hPa from NCEP/department of Energy (DOE) reanalysis II (Kanamitsu *et al.* 2002).

The MISO metrics introduced in this study was designed to represent larger fractional variance and to better capture the observed northward propagating ISO over the Asian summer monsoon (ASM) region than the RMM index after considerable sensitivity tests. Multivariate empirical orthogonal function (MV-EOF) analysis was applied to daily mean normalized OLR and 850-hPa zonal wind (U850) anomalies over the ASM region (10^{o}S-40^{o}N, 40^{o}-160^{o}E) from May 1st to September 30th in the 30 years of 1981-2010. The OLR and U850 anomalies were obtained from removing the first three harmonics in climatological annual cycle and removing the effect of interannual variation through subtracting last 120 day mean. After that, each of two anomaly fields were normalized by area averaged temporal standard deviation over the ASM region. The standard deviation used is 33.34 W m^{-2} for OLR and 4.02 m s^{-1} for U850. We do not apply filtering to define the index for monitoring and forecast purpose except 1-2-1 filtering. After applying the MV-EOF on the normalized OLR and U850 anomalies, we identified the first four modes as important components for representing ISO propagation over the ASM region. The first four PCs were defined as components of the MISO index. Percentage variance of each mode is 8.57, 5.49, 4.43, and 3.66% for the first, second, third, and fourth mode, respectively. Thus, the first four modes can account for 18.4% of total daily variance of the OLR and U850 anomalies over the ASM region.

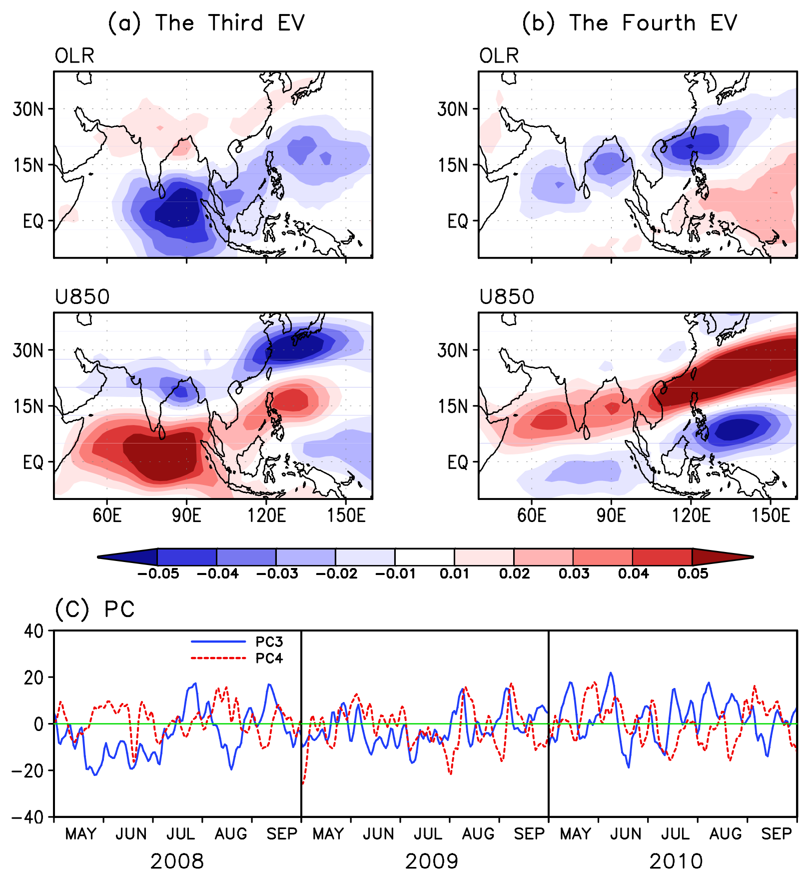

Fig.2 Same as Fig. 1 except for the third and fourth mode.

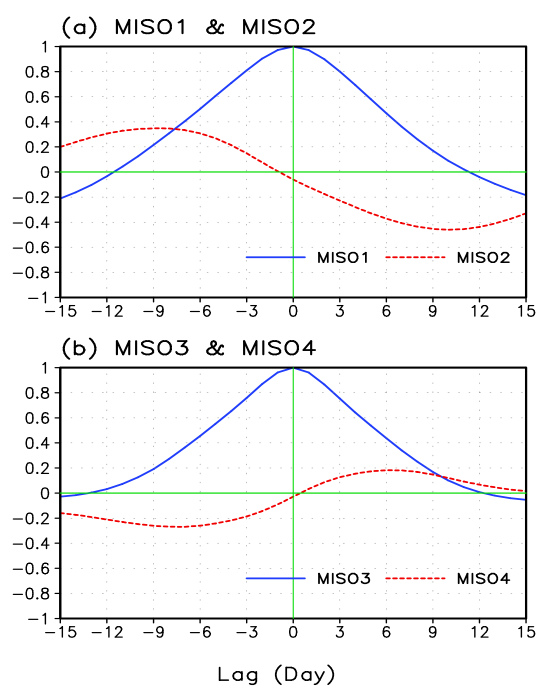

Fig. 3 Lead-lag correlations (a) between the MISO 1 and itself, and with MISO 2 and (b) between the MISO 3 and itself, and with MISO 4 during MJJAS.

3. Characteristics of the MISO Components

Figures 1 and 2 show the spatial distribution of eigen vector (EV) and principal component (PC) time series of the first four leading MV-EOF modes of the normalized OLR and

U850 anomalies. The first two MV-EOF modes together represent the dominant northward propagating ISO over the ASM region during entire warm season (Fig. 1) addressed in many previous studies (Waliser *et al.* 2003) and the third and fourth modes mainly capture the grand onset mode (LinHo and Wang 2002) of the ASM system (Fig. 2).

The first two EOF modes represent prominent northward propagating ISO over the entire ASM region which is typically oriented in a northwest-southeast direction (Fig. 1a and b). Power spectra of the PCs indicate that the bulk of the variance of the PCs is concentrated at intraseasonal periods (biweekly and 20-60 days). The northward propagating ISO is obvious with PC1 (or MISO1) lagging PC2 (or MISO2) by 7 to 12 days (Fig. 3a). The maximum correlation between MISO1 and MISO2 is -0.4 at a lag of 12 days. The RMM index captures the OLR variability primarily in the equatorial region whereas the MISO 1 and 2 capture large portion of the variability in the off-equatorial region, yielding more realistic variance pattern. Figure 4 shows the life cycle composite of the normalized OLR and 850-hPa wind anomalies using PC1 and PC2 phase space. It is noted that the MISO 1 and 2 describe better ISO variability center and represent better northward as well as eastward propagating pattern in the ASM region than the RMM.

This study demonstrates that the third and fourth MV-EOF modes are also important northward propagating ISO mode, particularly during early summer in association with the grand onset of the ASM system which was described by LinHo and Wang (2002). Differently from the first and second modes, OLR and wind anomalies are in phase over the Indian monsoon and West North Pacific-East Asian monsoon with a southwest-northeast tilt (Fig. 2a and b). Power spectra of the third and fourth PCs indicate that the bulk of their variance is concentrated at intraseasonal periods (biweekly and 20-40 days). The northward propagating ISO is

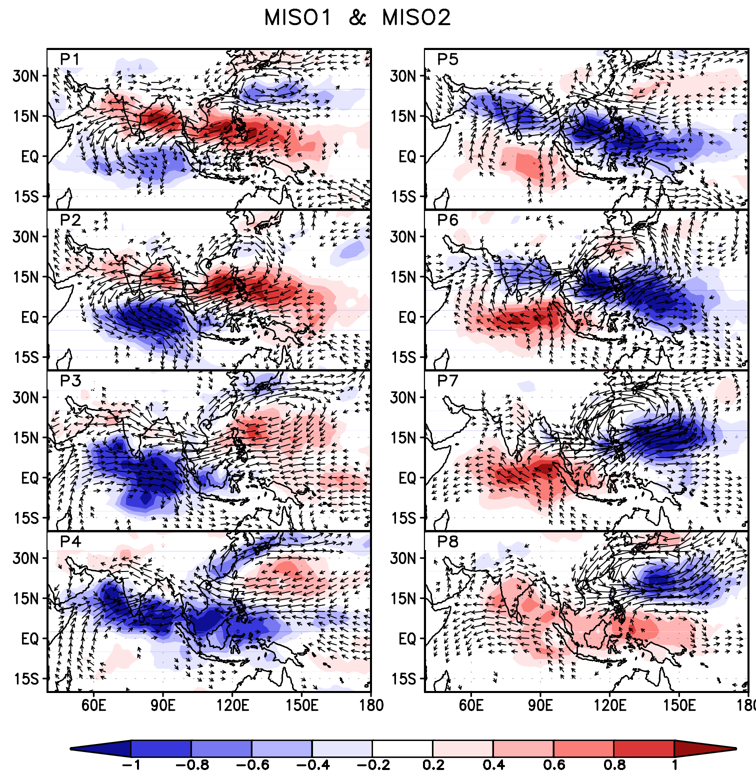

Fig. 4 The life cycle composite of pentad OLR (shading) and 850-hPa wind (vector) anomalies reconstructed based on the MISO1 and MISO2 in 8 phases.

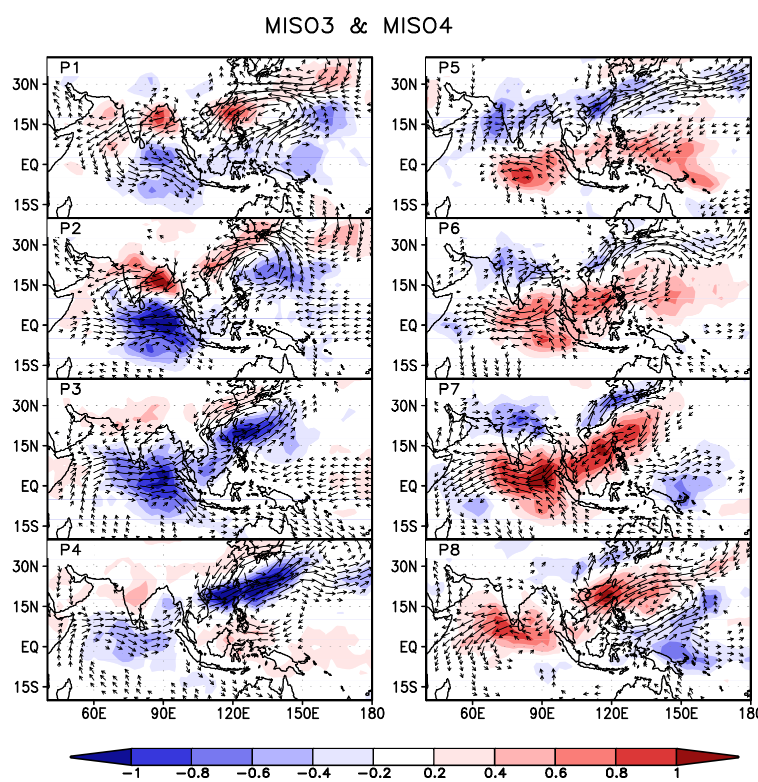

Fig. 5 Same as Fig. 4 except for MISO3 and MISO4.

obvious with PC4 (or MISO 4) lagging PC3 (or MISO 3) by 6 to 8 days (Fig. 3b). The maximum correlation between PC1 and PC2 is -0.28 at a lag of 7 days. The life cycle composite of the MISO 3 an MISO4 represents stepwise onset over the entire ASM region (Fig. 5).

4. Application to real-time monitoring

The northward-propagating MISO component can be monitored using the phase diagram between the MISO 1 and MISO 2 and between the MISO 3 and MISO 4 similar as the eastward-propagating MJO. Figure 6 show example of application to real-time monitoring. During late June to early December, the typical northward propagating ISO was dominant well represented by the points in the two-dimensional phase space defined by the MISO 2 and MISO 1 starting from June 17, 2006. Figure 6b well represents early onset and strong ISO activities over the East Asian monsoon region during early this summer of 2011.

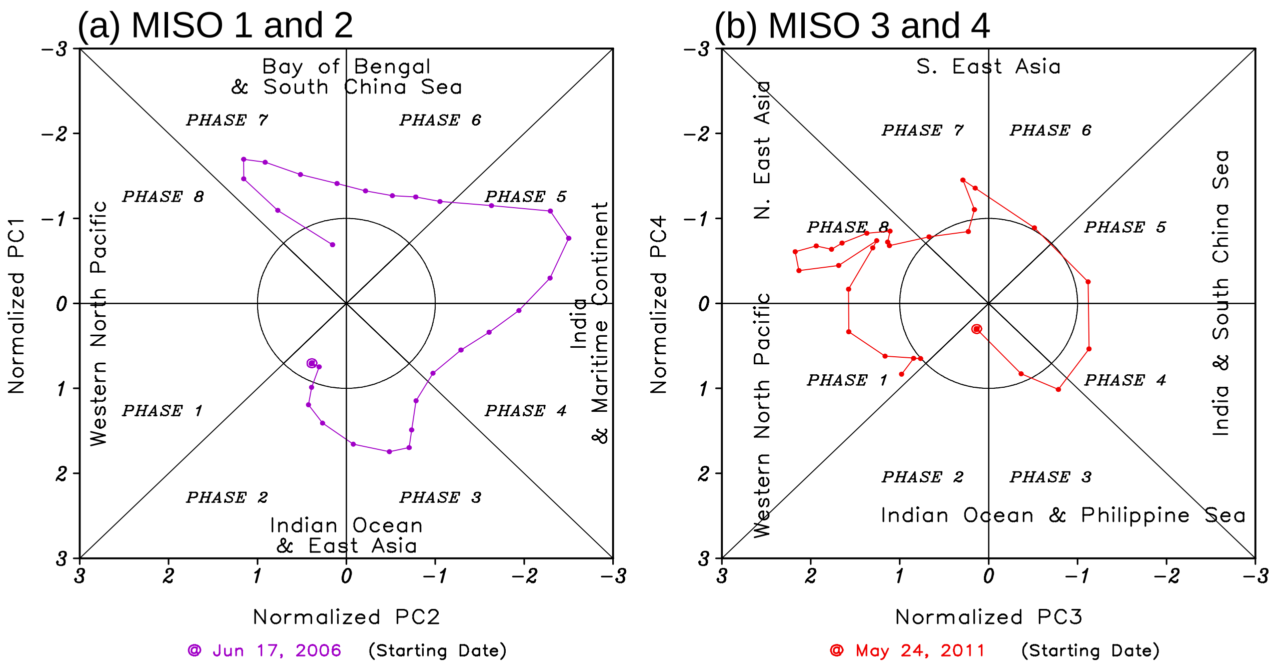

Fig. 6 (a) (MISO2, MISO1) phase space points starting from June 17, 2006. Eight defined regions of the phase space are labeled, as it the region considered to signify weak MISO activity. (b) same as (a) except for (MISO4, MISO3) phase space points starting from May 24, 2011.

5. Summary

Boreal summer Monsoon Intraseasonal Oscillation (MISO) is one of the most prominent short-term climate variability in the global monsoon system and more complex in nature than the Madden-Julian Oscillation (MJO) due to the interaction between the basic monsoon circulation and tropical ISO. To monitor and forecast MISO, we defined real-time multivariate MISO index using daily outgoing longwave radiation (OLR), zonal wind at 850 hPa (U850) over the Asian summer monsoon (ASM) region (10^{o}S-40^{o}N, 40^{o}-150^{o}E), differently from Real-time Multivariate MJO (RMM) index.

The RMM index captures the OLR variability primarily in the equatorial region whereas the new MISO index captures large portion of the variability in the off-equatorial region, yielding more realistic variance pattern. In addition, The MISO index describes ISO variability center better, captures more fractional variance and describes northward as well as eastward propagating pattern better in the ASM domain then RMM index. Sensitivity tests revealed that the MISO index with the first four modes using pentad OLR and U850 is most adequate in terms of fractional variance explained by the reconstructed field and ability to capture the northward propagating MISO.

The northward-propagating MISO component can be monitored using the phase diagram between the first and second PC similar as the eastward-propagating MJO. Taking into account distinct regional characteristics of MISO with smaller horizontal scale than MJO, the reconstructed field from the first four modes may provide more useful information.

References

Kajikawa, Y. and T. Yasunari T, 2005: Interannual variability of the 10-25- and 30-60-day variation over the South China Sea during boreal summer. *Geophys. Res. Lett.*, **32**, L04710, doi:10.1029/2004GL021836.

Kanamitsu, M., and Coauthors, 2002: NCEP dynamical seasonal forecast system 2000. *Bull. Am. Meteor. Soc.*, **83**, 1019-1037.

Lau, W. K. M., and D. E. Waliser (Eds.), 2005: *Intraseasonal Variability of the Atmosphere-Ocean Climate System*, Springer-Verlag, 474 pp.

Liebmann, B., and C. A. Smith, 1996: Description of a complete (interpolated) outgoing longwave radiation dataset. Bull Am Meteor Soc 77:1275-1277.

LinHo, and B. Wang, 2002: The time-space structure of the Asian-Pacific summer monsoon: a fast annual cycle view. *J. Climate*, **15**, 2001-2019.

Madden, R. A., 1986: Seasonal-variations of the 40–50 day oscillation in the tropics. *J Atmos Sci.*, **43**, 3138–3158.

Madden, R. A., and P. R. Julian, 1972: Description of global-scale circulation cells in tropics with a 40-50day period. *J. Atmos Sci.*, **29**, 1109-1123.

Madden, R. A., and P. R. Julian, 1994: Observations of the 40-50-Day Tropical Oscillation - a Review. *Mon. Wea. Rev.*, **122**, 814-837.

Waliser, D.E., W. Stern, S. Schubert, and K. M. Lau, 2003: Dynamic predictability of intraseasonal variability associated with the Asian summer monsoon. *Quart. J. Roy. Meteor. Soc.*, **129**, 2897-2925.

Wang, B., 2006: *The Asian monsoon*. Springer-Verlag, 787 pp.

Wang, B., and H. Rui, 1990: Synoptic climatology of trans ient tropical intraseasonal convection anomalies: 1975-1985. *Meteor. Atmos. Phys.*, **44**, 43-61.

Webster, P. J., and C. Hoyos, 2004: Prediction of monsoon rainfall and river discharge on 15-30 day time sclaes. *Bull. Amer. Met. Soc.*, **85**, 1745-1769.

Webster, P. J., and Coauthors, 1998: Monsoon: Processes, predictability and the prospects for prediction. *J. Geophys. Res.*, **103**, 13341-1451.

Wheeler, M. C., and H. H. Hendon, 2004: An all-season real-time multivariate MJO index: Development of an index for monitoring and prediction. *Mon. Wea. Rev.*, **132**,1917-1932.

Yasunari, T., 1979: Cloudiness fluctuations associated with the northern hemisphere summer monsoon. *J. Meteor. Soc. Japan*, **57**, 227-242.

Yasunari, T., 1980: A quasi-stationary appearance of 30 to 40 day period in the cloudiness fluctuation during the summer monsoon over India. *J. Meteorol. Soc. Japan*, **58**, 225-229.